

Measurement of masses of $\Xi_c(2645)$ and $\Xi_c(2815)$ baryons

K. Abe,⁹ K. Abe,⁴⁹ N. Abe,⁵² I. Adachi,⁹ H. Aihara,⁵¹ D. Anipko,¹ K. Aoki,²⁵
 K. Arinstein,¹ Y. Asano,⁵⁶ T. Aso,⁵⁵ V. Aulchenko,¹ T. Aushev,¹⁵ T. Aziz,⁴⁷ S. Bahinipati,⁴
 A. M. Bakich,⁴⁶ V. Balagura,¹⁵ Y. Ban,³⁷ S. Banerjee,⁴⁷ E. Barberio,²⁴ M. Barbero,⁸
 A. Bay,²¹ I. Bedny,¹ K. Belous,¹⁴ U. Bitenc,¹⁶ I. Bizjak,¹⁶ S. Blyth,²⁷ A. Bondar,¹
 A. Bozek,³⁰ M. Bračko,^{9,23,16} J. Brodzicka,³⁰ T. E. Browder,⁸ M.-C. Chang,⁵⁰ P. Chang,²⁹
 Y. Chao,²⁹ A. Chen,²⁷ K.-F. Chen,²⁹ W. T. Chen,²⁷ B. G. Cheon,³ R. Chistov,¹⁵
 J. H. Choi,¹⁸ S.-K. Choi,⁷ Y. Choi,⁴⁵ Y. K. Choi,⁴⁵ A. Chuvikov,³⁹ S. Cole,⁴⁶ J. Dalseno,²⁴
 M. Danilov,¹⁵ M. Dash,⁵⁷ R. Dowd,²⁴ J. Dragic,⁹ A. Drutskoy,⁴ S. Eidelman,¹ Y. Enari,²⁵
 D. Epifanov,¹ F. Fang,⁸ S. Fratina,¹⁶ H. Fujii,⁹ M. Fujikawa,²⁶ N. Gabyshev,¹
 A. Garmash,³⁹ T. Gershon,⁹ A. Go,²⁷ G. Gokhroo,⁴⁷ P. Goldenzweig,⁴ B. Golob,^{22,16}
 A. Gorišek,¹⁶ M. Grosse Perdekamp,^{11,40} H. Guler,⁸ H. Ha,¹⁸ J. Haba,⁹ K. Hara,⁹
 T. Hara,³⁵ Y. Hasegawa,⁴⁴ N. C. Hastings,⁵¹ K. Hayasaka,²⁵ H. Hayashii,²⁶ M. Hazumi,⁹
 D. Heffernan,³⁵ T. Higuchi,⁹ L. Hinz,²¹ T. Hojo,³⁵ T. Hokuue,²⁵ Y. Hoshi,⁴⁹ K. Hoshina,⁵⁴
 S. Hou,²⁷ W.-S. Hou,²⁹ Y. B. Hsiung,²⁹ Y. Igarashi,⁹ T. Iijima,²⁵ K. Ikado,²⁵ A. Imoto,²⁶
 K. Inami,²⁵ A. Ishikawa,⁵¹ H. Ishino,⁵² K. Itoh,⁵¹ R. Itoh,⁹ M. Iwasaki,⁵¹ Y. Iwasaki,⁹
 C. Jacoby,²¹ M. Jones,⁸ R. Kagan,¹⁵ H. Kakuno,⁵¹ J. H. Kang,⁵⁸ J. S. Kang,¹⁸
 P. Kapusta,³⁰ S. U. Kataoka,²⁶ N. Katayama,⁹ H. Kawai,² T. Kawasaki,³² N. Kent,⁸
 H. R. Khan,⁵² A. Kibayashi,⁵² H. Kichimi,⁹ H. J. Kim,²⁰ H. O. Kim,⁴⁵ J. H. Kim,⁴⁵
 S. K. Kim,⁴³ T. H. Kim,⁵⁸ Y. J. Kim,⁶ K. Kinoshita,⁴ N. Kishimoto,²⁵ S. Korpar,^{23,16}
 Y. Kozakai,²⁵ P. Križan,^{22,16} P. Krokovny,⁹ T. Kubota,²⁵ R. Kulasiri,⁴ R. Kumar,³⁶
 C. C. Kuo,²⁷ H. Kurashiro,⁵² E. Kurihara,² A. Kusaka,⁵¹ A. Kuzmin,¹ Y.-J. Kwon,⁵⁸
 J. S. Lange,⁵ G. Leder,¹³ J. Lee,⁴³ S. E. Lee,⁴³ Y.-J. Lee,²⁹ T. Lesiak,³⁰ J. Li,⁴²
 A. Limosani,⁹ S.-W. Lin,²⁹ Y. Liu,⁶ D. Liventsev,¹⁵ J. MacNaughton,¹³ G. Majumder,⁴⁷
 F. Mandl,¹³ D. Marlow,³⁹ H. Matsumoto,³² T. Matsumoto,⁵³ A. Matyja,³⁰ S. McOnie,⁴⁶
 Y. Mikami,⁵⁰ W. Mitaroff,¹³ K. Miyabayashi,²⁶ H. Miyake,³⁵ H. Miyata,³² Y. Miyazaki,²⁵
 R. Mizuk,¹⁵ D. Mohapatra,⁵⁷ G. R. Moloney,²⁴ T. Mori,⁵² J. Mueller,³⁸ A. Murakami,⁴¹
 T. Nagamine,⁵⁰ Y. Nagasaka,¹⁰ T. Nakagawa,⁵³ I. Nakamura,⁹ E. Nakano,³⁴ M. Nakao,⁹
 H. Nakazawa,⁹ Z. Natkaniec,³⁰ K. Neichi,⁴⁹ S. Nishida,⁹ O. Nitoh,⁵⁴ S. Noguchi,²⁶
 T. Nozaki,⁹ A. Ogawa,⁴⁰ S. Ogawa,⁴⁸ T. Ohshima,²⁵ T. Okabe,²⁵ S. Okuno,¹⁷ S. L. Olsen,⁸
 S. Ono,⁵² Y. Onuki,³² W. Ostrowicz,³⁰ H. Ozaki,⁹ P. Pakhlov,¹⁵ G. Pakhlova,¹⁵ H. Palka,³⁰
 C. W. Park,⁴⁵ H. Park,²⁰ K. S. Park,⁴⁵ N. Parslow,⁴⁶ L. S. Peak,⁴⁶ M. Pernicka,¹³
 R. Pestotnik,¹⁶ M. Peters,⁸ L. E. Piilonen,⁵⁷ A. Poluektov,¹ F. J. Ronga,⁹ N. Root,¹
 M. Rozanska,³⁰ S. Saitoh,⁹ Y. Sakai,⁹ H. Sakamoto,¹⁹ H. Sakaue,³⁴ T. R. Sarangi,⁶
 N. Sato,²⁵ N. Satoyama,⁴⁴ K. Sayeed,⁴ T. Schietinger,²¹ O. Schneider,²¹ P. Schönmeier,⁵⁰
 J. Schümann,²⁸ C. Schwanda,¹³ A. J. Schwartz,⁴ R. Seidl,^{11,40} T. Seki,⁵³ K. Senyo,²⁵
 M. E. Sevier,²⁴ M. Shapkin,¹⁴ Y.-T. Shen,²⁹ T. Shibata,³² H. Shibuya,⁴⁸ B. Shwartz,¹
 V. Sidorov,¹ J. B. Singh,³⁶ A. Sokolov,¹⁴ A. Somov,⁴ N. Soni,³⁶ R. Stamen,⁹ S. Stanič,³³
 M. Starič,¹⁶ H. Stoeck,⁴⁶ A. Sugiyama,⁴¹ K. Sumisawa,³⁵ T. Sumiyoshi,⁵³ S. Suzuki,⁴¹
 S. Y. Suzuki,⁹ O. Tajima,⁹ N. Takada,⁴⁴ F. Takasaki,⁹ K. Tamai,⁹ N. Tamura,³²
 K. Tanabe,⁵¹ M. Tanaka,⁹ G. N. Taylor,²⁴ Y. Teramoto,³⁴ X. C. Tian,³⁷ I. Tikhomirov,¹⁵

K. Trabelsi,⁸ Y. F. Tse,²⁴ T. Tsuboyama,⁹ T. Tsukamoto,⁹ K. Uchida,⁸ Y. Uchida,⁶
 S. Uehara,⁹ T. Uglov,¹⁵ K. Ueno,²⁹ Y. Unno,⁹ S. Uno,⁹ P. Urquijo,²⁴ Y. Ushiroda,⁹
 Y. Usov,¹ G. Varner,⁸ K. E. Varvell,⁴⁶ S. Villa,²¹ C. C. Wang,²⁹ C. H. Wang,²⁸
 M.-Z. Wang,²⁹ M. Watanabe,³² Y. Watanabe,⁵² J. Wicht,²¹ L. Widhalm,¹³
 J. Wiechczynski,³⁰ E. Won,¹⁸ C.-H. Wu,²⁹ Q. L. Xie,¹² B. D. Yabsley,⁴⁶ A. Yamaguchi,⁵⁰
 H. Yamamoto,⁵⁰ S. Yamamoto,⁵³ Y. Yamashita,³¹ M. Yamauchi,⁹ Heyoung Yang,⁴³
 J. Ying,³⁷ S. Yoshino,²⁵ Y. Yuan,¹² Y. Yusa,⁵⁷ S. L. Zang,¹² C. C. Zhang,¹² J. Zhang,⁹
 L. M. Zhang,⁴² Z. P. Zhang,⁴² V. Zhilich,¹ T. Ziegler,³⁹ A. Zupanc,¹⁶ and D. Zürcher²¹

(The Belle Collaboration)

¹*Budker Institute of Nuclear Physics, Novosibirsk*

²*Chiba University, Chiba*

³*Chonnam National University, Kwangju*

⁴*University of Cincinnati, Cincinnati, Ohio 45221*

⁵*University of Frankfurt, Frankfurt*

⁶*The Graduate University for Advanced Studies, Hayama, Japan*

⁷*Gyeongsang National University, Chinju*

⁸*University of Hawaii, Honolulu, Hawaii 96822*

⁹*High Energy Accelerator Research Organization (KEK), Tsukuba*

¹⁰*Hiroshima Institute of Technology, Hiroshima*

¹¹*University of Illinois at Urbana-Champaign, Urbana, Illinois 61801*

¹²*Institute of High Energy Physics,*

Chinese Academy of Sciences, Beijing

¹³*Institute of High Energy Physics, Vienna*

¹⁴*Institute of High Energy Physics, Protvino*

¹⁵*Institute for Theoretical and Experimental Physics, Moscow*

¹⁶*J. Stefan Institute, Ljubljana*

¹⁷*Kanagawa University, Yokohama*

¹⁸*Korea University, Seoul*

¹⁹*Kyoto University, Kyoto*

²⁰*Kyungpook National University, Taegu*

²¹*Swiss Federal Institute of Technology of Lausanne, EPFL, Lausanne*

²²*University of Ljubljana, Ljubljana*

²³*University of Maribor, Maribor*

²⁴*University of Melbourne, Victoria*

²⁵*Nagoya University, Nagoya*

²⁶*Nara Women's University, Nara*

²⁷*National Central University, Chung-li*

²⁸*National United University, Miao Li*

²⁹*Department of Physics, National Taiwan University, Taipei*

³⁰*H. Niewodniczanski Institute of Nuclear Physics, Krakow*

³¹*Nippon Dental University, Niigata*

³²*Niigata University, Niigata*

³³*University of Nova Gorica, Nova Gorica*

³⁴*Osaka City University, Osaka*

³⁵*Osaka University, Osaka*

³⁶*Panjab University, Chandigarh*

- ³⁷*Peking University, Beijing*
- ³⁸*University of Pittsburgh, Pittsburgh, Pennsylvania 15260*
- ³⁹*Princeton University, Princeton, New Jersey 08544*
- ⁴⁰*RIKEN BNL Research Center, Upton, New York 11973*
- ⁴¹*Saga University, Saga*
- ⁴²*University of Science and Technology of China, Hefei*
- ⁴³*Seoul National University, Seoul*
- ⁴⁴*Shinshu University, Nagano*
- ⁴⁵*Sungkyunkwan University, Suwon*
- ⁴⁶*University of Sydney, Sydney NSW*
- ⁴⁷*Tata Institute of Fundamental Research, Bombay*
- ⁴⁸*Toho University, Funabashi*
- ⁴⁹*Tohoku Gakuin University, Tagajo*
- ⁵⁰*Tohoku University, Sendai*
- ⁵¹*Department of Physics, University of Tokyo, Tokyo*
- ⁵²*Tokyo Institute of Technology, Tokyo*
- ⁵³*Tokyo Metropolitan University, Tokyo*
- ⁵⁴*Tokyo University of Agriculture and Technology, Tokyo*
- ⁵⁵*Toyama National College of Maritime Technology, Toyama*
- ⁵⁶*University of Tsukuba, Tsukuba*
- ⁵⁷*Virginia Polytechnic Institute and State University, Blacksburg, Virginia 24061*
- ⁵⁸*Yonsei University, Seoul*

Abstract

We report a precise measurement of masses of the $\Xi_c(2645)$ and $\Xi_c(2815)$ baryons using data collected by the Belle experiment at the KEKB e^+e^- collider. The states $\Xi_c(2645)^{0,+}$ are observed in the $\Xi_c^{+,0}\pi^{-,+}$ decay modes, while the $\Xi_c(2815)^{0,+}$ are reconstructed in the $\Xi_c(2645)^{+,0}\pi^{-,+}$ decay modes.

PACS numbers: 14.40.Lb, 13.25.Ft, 13.25.Gv, 13.20.Jf

INTRODUCTION

The study of charmed baryons has recently been the focus of significant experimental effort [1, 2, 3, 4, 5]. Several new excited states have been observed or their properties determined for the first time, enabling tests of quark (and other) models and predictions of heavy quark symmetry [6, 7].

This paper presents the measurement of exclusive decays of $\Xi_c(2645)^0$, $\Xi_c(2645)^+$, $\Xi_c(2815)^0$ and $\Xi_c(2815)^+$ baryons [8] and determination of their masses. The states $\Xi_c(2645)^0$ and $\Xi_c(2645)^+$ are reconstructed in $\Xi_c^+\pi^-$ and $\Xi_c^0\pi^+$ decay modes, respectively. For the hyperons $\Xi_c(2815)^0$ and $\Xi_c(2815)^+$, the decays into $\Xi_c(2645)^+\pi^-$ and $\Xi_c(2645)^0\pi^+$ are observed for the first time and used to precisely determine their masses. The world averages of masses, relevant for this study, are shown in Table I (as given by the Particle Data Group (PDG) [9]). Similar precisions are achieved in the determination of the respective mass splittings within isospin doublets. More precise determination of the masses of $\Xi_c(2645)^{+,0}$ and $\Xi_c(2815)^{+,0}$ are required.

This article is organized as follows. The next two sections describe the data sample and the reconstruction of Ξ_c baryons, respectively. The final two sections are devoted to the mass determination of the $\Xi_c(2645)$ and $\Xi_c(2815)$, respectively.

TABLE I: Masses of hyperons Ξ_c , $\Xi_c(2645)$ and $\Xi_c(2815)$, as given by the Particle Data Group [9].

Particle	Mass [MeV/c ²]
Ξ_c^+	$2467.6_{-1.0}^{+0.4}$ (average) 2468.0 ± 0.4 (fit)
Ξ_c^0	$2471.09_{-1.00}^{+0.35}$ (average) 2471.0 ± 0.6 (fit)
$\Xi_c(2645)^+$	2646.6 ± 1.5
$\Xi_c(2645)^0$	2646.2 ± 1.2
$\Xi_c(2815)^+$	2816.6 ± 1.2
$\Xi_c(2815)^0$	2818.2 ± 2.2

DETECTOR AND DATA SAMPLE

The data used for this study were collected on the $\Upsilon(4S)$ resonance using the Belle detector at the KEKB asymmetric e^+e^- collider [10]. The integrated luminosity of the data sample is 414 fb^{-1} .

The Belle detector is a large-solid-angle magnetic spectrometer that consists of a silicon vertex detector (SVD), a 50-layer central drift chamber (CDC), an array of aerogel threshold Čerenkov counters (ACC), a barrel-like arrangement of time-of-flight scintillation counters (TOF), and an electromagnetic calorimeter comprised of CsI(Tl) crystals (ECL) located inside a super-conducting solenoid coil that provides a 1.5 T magnetic field. An iron flux-return located outside of the coil is instrumented to detect K_L^0 mesons and to identify muons (KLM). A detailed description of the Belle detector can be found elsewhere [11].

RECONSTRUCTION

Reconstruction of Ξ_c , $\Xi_c(2645)$ and $\Xi_c(2815)$ decays for this analysis proceeds in three steps: reconstruction of tracks and their identification as protons, kaons or pions; combination of tracks to reconstruct Λ and Ξ^- hyperons; and the selection of Ξ_c candidates from combinations of tracks and hyperons. The method for each step is described in the following sections in turn.

Track reconstruction and identification

Charged tracks are reconstructed from hits in the CDC using a Kalman filter [12], and matched to hits in the SVD where present. Quality criteria are then applied. All tracks other than those used to form Λ and Ξ^- candidates, are required to have impact parameters relative to the interaction point (IP) of less than 0.5 cm in the $r - \phi$ plane, and 5 cm in the z direction [13]. The transverse momentum of each track is required to exceed 0.1 GeV/ c , in order to reduce the low momentum combinatorial background.

Hadron identification is based on information from the CDC (energy loss dE/dx), TOF and ACC, combined to form likelihoods $\mathcal{L}(p)$, $\mathcal{L}(K)$ and $\mathcal{L}(\pi)$ for the proton, kaon and pion hypotheses, respectively. These likelihoods are combined to form ratios $\mathcal{P}(K/\pi) = \mathcal{L}(K)/(\mathcal{L}(K) + \mathcal{L}(\pi))$ and $\mathcal{P}(p/K) = \mathcal{L}(p)/(\mathcal{L}(p) + \mathcal{L}(K))$, spanning the range from zero to one, which are then used to identify individual tracks [11]. Kaon candidates are required to satisfy $\mathcal{P}(K/\pi) > 0.9$ and $\mathcal{P}(p/K) < 0.98$; the second criterion is to veto protons. For illustration, this selection has an efficiency of around 80% and a probability of misidentification of a pion as a kaon of around 3.8%. Protons are required to satisfy $\mathcal{P}(p/K) > 0.9$. Pion candidates, except those coming from the decay of the Λ hyperon, should satisfy both a proton and a kaon veto: $\mathcal{P}(p/K) < 0.98$ and $\mathcal{P}(K/\pi) < 0.98$.

Electrons are identified using a similar likelihood ratio $\mathcal{P}_e = \mathcal{L}_e/(\mathcal{L}_e + \mathcal{L}_{\text{non-}e})$, based on a combination of dE/dx measurements in the CDC, the response of the ACC, E/p , where p is the momentum of the track and E the energy of the associated cluster in the ECL, as well as matching between the track and the ECL cluster position and the transverse shower shape. All tracks with $\mathcal{P}_e > 0.98$ are assumed to be electrons, and removed from the proton, kaon and pion samples.

Reconstruction of Λ and Ξ^-

We reconstruct Λ hyperons in the $\Lambda \rightarrow p\pi^-$ decay mode, requiring the proton track to satisfy $\mathcal{P}(p/K) > 0.1$ [14], and fitting the p and π tracks to a common vertex. To reduce the number of poorly reconstructed candidates, the $\chi^2/n.d.f.$ of the vertex should not exceed 25 (removing approximately 2% of candidates) and the difference in the z -coordinate between the proton and pion at the vertex is required to be less than 2 cm. Due to the large $c\tau$ factor for Λ hyperons (7.89 cm), we demand that the distance between the decay vertex and the IP in the $r - \phi$ plane be greater than 1 cm. The invariant mass of the proton-pion pair is required to be within 2.4 MeV/ c^2 (≈ 2.5 standard deviations) of the nominal Λ mass. The mean value of the Λ signal in the reconstructed mass distribution was found to be 1115.7 ± 0.1 MeV/ c^2 , in agreement with the world average value [9].

In accordance with the above, we reconstruct Ξ^- hyperons in the decay mode $\Xi^- \rightarrow \Lambda\pi^-$.

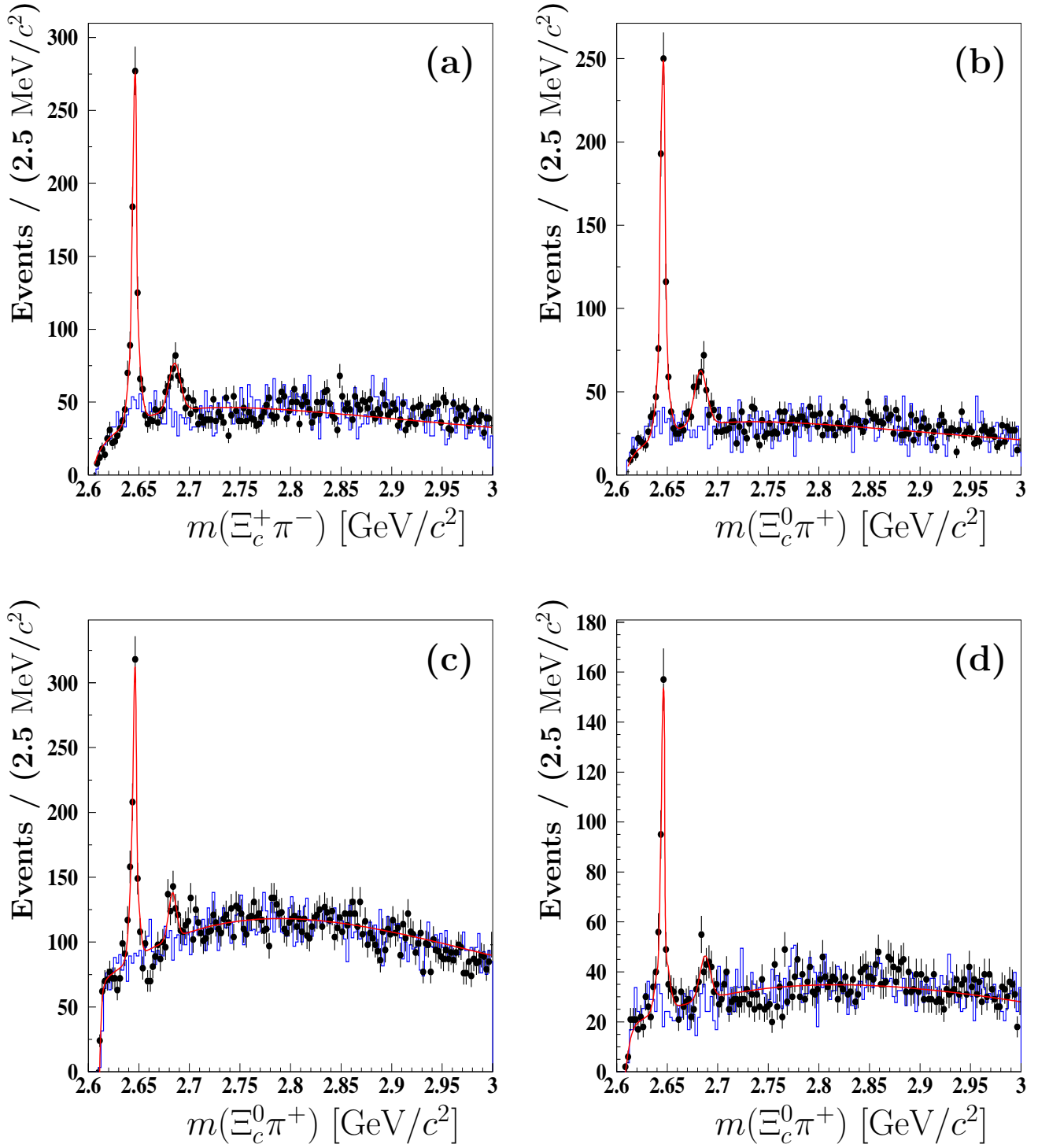


FIG. 1: Invariant mass distributions for (a) $\Xi_c^+ \pi^-$ ($\Xi_c^+ \rightarrow \Xi^- \pi^+ \pi^+$), (b) $\Xi_c^0 \pi^+$ ($\Xi_c^0 \rightarrow \Xi^- \pi^+$), (c) $\Xi_c^0 \pi^+$ ($\Xi_c^0 \rightarrow \Lambda K^- \pi^+$) and (d) $\Xi_c^0 \pi^+$ ($\Xi_c^0 \rightarrow p K^- K^- \pi^+$). Curves are the results of the fit. The histograms correspond to the Ξ_c mass sidebands.

The Λ and π candidates are fitted to a common vertex, whose $\chi^2/n.d.f.$ is required to be at most 25 (removing approximately 2% of candidates). The distance between the Ξ^- decay vertex position and IP in the $r - \phi$ plane should be at least 5 mm, and less than the corresponding distance between the IP and the Λ vertex. The invariant mass of the $\Lambda\pi^-$ pair is required to be within $7.5 \text{ MeV}/c^2$ of the nominal value (≈ 2.5 standard deviations). The mass of the Ξ^- was found to be $1321.78 \pm 0.21 \text{ MeV}/c^2$, in agreement with the PDG average: $1321.34 \pm 0.14 \text{ MeV}/c^2$ [9].

Reconstruction of Ξ_c , $\Xi_c(2645)$ and $\Xi_c(2815)$

The reconstructed Λ and Ξ^- candidates and the remaining charged hadrons in an event are combined to form candidates for the charged Ξ_c decay,

$$\Xi_c^+ \rightarrow \Xi^- \pi^+ \pi^+ \quad (1)$$

and three decays of the neutral state,

$$\Xi_c^0 \rightarrow \Xi^- \pi^+ \quad (2)$$

$$\Xi_c^0 \rightarrow \Lambda K^- \pi^+ \quad (3)$$

$$\Xi_c^0 \rightarrow p K^- K^- \pi^+. \quad (4)$$

The signal region of the Ξ_c is defined by the reconstructed mass windows (2.455–2.485) GeV/c^2 for (1), (2.45–2.49) GeV/c^2 for (2) and (2.46–2.48) GeV/c^2 for final states (3) and (4).

All particles forming the Ξ_c candidate are fitted to a common vertex constraining their invariant mass to the values given in Table I. A goodness-of-fit criterion is applied: $\chi^2/n.d.f. < 50$ (removing approximately 5% of candidates). A strong Ξ_c signal is observed in the invariant mass distributions of each of the decays studied. Taking into account efficiencies, estimated from the simulated Monte Carlo samples, the relative branching fractions of the respective Ξ_c decays are found to be in agreement with the values determined in Ref. [5].

The decays $\Xi_c(2645)^0 \rightarrow \Xi_c^+ \pi^-$ and $\Xi_c(2645)^+ \rightarrow \Xi_c^0 \pi^+$ are reconstructed by fitting pairs of charged pions and Ξ_c candidates to a common vertex. The combinations are accepted if they satisfy the criterion $\chi^2/n.d.f. < 10$ (removing approximately 10% of candidates) and if the momentum of the $\Xi_c\pi$ system in the center-of-mass system (CMS) exceeds $2.5 \text{ GeV}/c$. Due to the hard momentum spectrum of baryons produced in e^+e^- processes, this requirement significantly suppresses the combinatorial background.

A clear $\Xi_c(2645)$ baryon signal is observed in the $\Xi_c\pi$ invariant mass distributions for all four decays of the Ξ_c (Fig. 1). In addition, a second less pronounced and broader maximum is observed in the mass region between 2.66 and 2.7 GeV/c^2 . Its origin was traced using Monte Carlo samples to exclusive decays of higher excitations of Ξ_c hyperons. It was found that the overall characteristics of this second signal are reasonably well reproduced (Fig. 2) assuming the following decay chain: $\Xi_c(2790) \rightarrow \Xi_c'(2579)\pi$, $\Xi_c' \rightarrow \Xi_c\gamma$. In the reconstruction the photon is missed and the Ξ_c and π invariant mass is peaked around $2.68 \text{ GeV}/c^2$. Fits to the mass distributions in different decay modes yield a mass of this excess from 2683 MeV/c^2 to 2687 MeV/c^2 with a width between 3.5 MeV and 5.3 MeV. These values are in agreement with MC expectations.

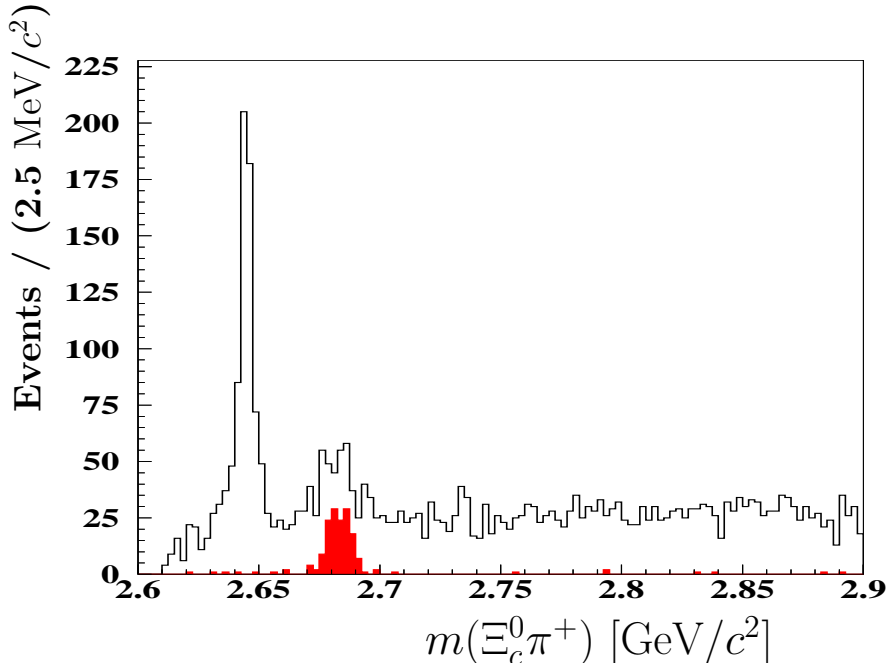


FIG. 2: Invariant mass distribution of selected $\Xi_c^0\pi^+$ ($\Xi_c^0 \rightarrow \Xi^- \pi^+$) combinations (open histogram) together with expected contribution from the decay $\Xi_c(2790) \rightarrow \Xi_c'(2579)\pi$, $\Xi_c' \rightarrow \Xi_c\gamma$, determined from Monte Carlo simulation (shaded histogram).

Next the decays $\Xi_c(2815)^0 \rightarrow \Xi_c(2645)^+\pi^-$ and $\Xi_c(2815)^+ \rightarrow \Xi_c(2645)^0\pi^+$ are reconstructed by fitting the $\Xi_c(2645)$ candidates and an additional charged pion to a common vertex. The combinations are accepted if they satisfy the criterion $\chi^2/n.d.f. < 10$ (removing approximately 10% of candidates), and if the momentum of the $\Xi_c(2645)\pi$ system in the CMS exceeds $2.5 \text{ GeV}/c$. The signal region for the $\Xi_c(2645)$ is defined as $(2.635\text{--}2.655) \text{ GeV}/c^2$ for all four decay chains studied. A $\Xi_c(2815)$ baryon signal is observed in the $\Xi_c(2645)\pi$ invariant mass distributions for all four decays of the Ξ_c (Fig. 3).

Again a second, broader maximum is observed in the mass region around $2.97 \text{ GeV}/c^2$ in the invariant mass of $\Xi_c(2645)^+\pi^-$ pairs. It is assumed to originate from exclusive decays of higher excitations of charmed-strange hyperons, observed in Ref. [1].

$\Xi_c(2645)$ MASS DETERMINATION

For each decay mode, we extract the signal yield and the $\Xi_c(2645)$ mass and width from a fit to the invariant mass distribution of $\Xi_c\pi$ pairs. We use two Gaussians with a common mean for the signal of the $\Xi_c(2645)$:

$$\mathcal{P}_s(m; \mu, \sigma_1, \sigma_2, f_1) = f_1\mathcal{G}(m; \mu, \sigma_1) + (1 - f_1)\mathcal{G}(m; \mu, \sigma_2), \quad (5)$$

and a single Gaussian $\mathcal{G}_f(m; \mu_f, \sigma_f)$ for the feed-down due to the $\Xi_c(2790)$. The background for channels (1) and (2) is described by a threshold function

$$\mathcal{T}(m, m_0) = \sqrt{m - m_0}, \quad (6)$$

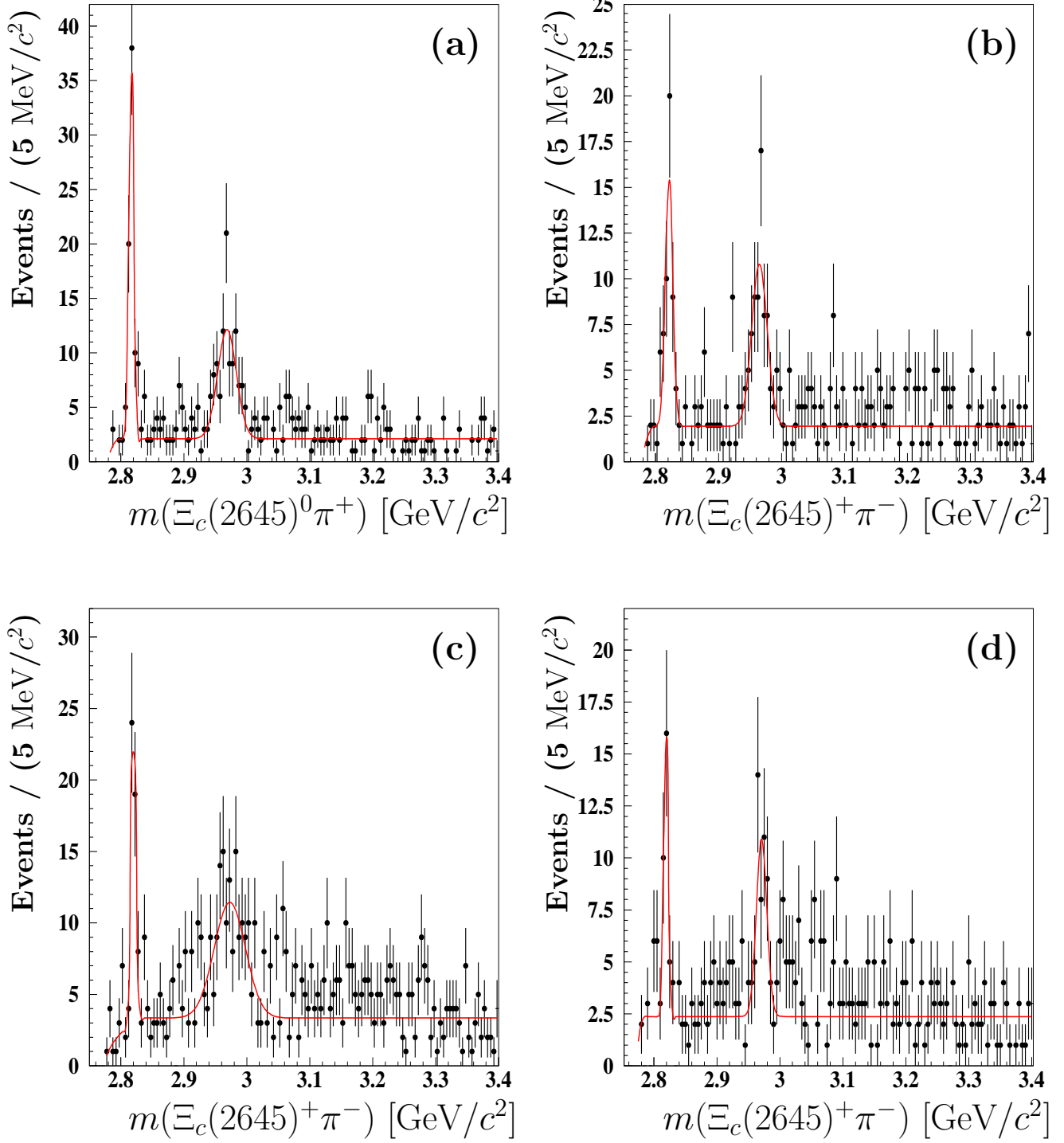


FIG. 3: Invariant mass distributions for (a) $\Xi_c(2645)^0\pi^+$ ($\Xi_c(2645)^0 \rightarrow \Xi_c^+\pi^-, \Xi_c^+ \rightarrow \Xi^-\pi^+\pi^+$), (b) $\Xi_c(2645)^+\pi^-$ ($\Xi_c(2645)^+ \rightarrow \Xi_c^0\pi^+, \Xi_c^0 \rightarrow \Xi^-\pi^+$), (c) $\Xi_c(2645)^+\pi^-$ ($\Xi_c(2645)^+ \rightarrow \Xi_c^0\pi^+, \Xi_c^0 \rightarrow \Lambda K^-\pi^+$) and (d) $\Xi_c(2645)^+\pi^-$ ($\Xi_c(2645)^+ \rightarrow \Xi_c^0\pi^+, \Xi_c^0 \rightarrow pK^-K^-\pi^+$). Curves are the results of the fit. The histograms correspond to the Ξ_c mass sidebands.

(where m_0 corresponds to the threshold's mass value) multiplied by a 4th order polynomial p_4 with coefficients $c_i, i = 0, 1, \dots, 4$:

$$\mathcal{P}_b(m; m_0, c_0, c_1, c_2, c_3, c_4) = \mathcal{T}p_4. \quad (7)$$

For channels (3) and (4), the background shape in the threshold region is better described by the function

$$\mathcal{P}_b(m; m_0, a) = \frac{1}{1 + e^{-a(m-m_0)}}, \quad (8)$$

where a is a free parameter to be determined by the fit. Thus the overall fit parameterization reads

$$\mathcal{P} = c_s\mathcal{P}_s + c_f\mathcal{G}_f + c_b\mathcal{P}_b, \quad (9)$$

where the yields c_s, c_f and c_b are to be determined from the fit. Other parameters determined by the fit are $\mu, \sigma_1, \sigma_2, f_1, \mu_f$ and σ_f .

The shape of the background function, is fixed from the fit to the spectrum of $\Xi_c\pi$ invariant masses using the mass sideband Ξ_c candidates: (2.37–2.41) GeV/ c^2 and (2.52–2.57) GeV/ c^2 . Results of the fits are summarized in Table II. The values of the $\Xi_c(2645)$ mass determined from each decay channel agree within one standard deviation.

TABLE II: Signal yields and $\Xi_c(2645)$ masses and widths, obtained from the fits to the $\Xi_c\pi$ mass spectra for the Ξ_c decays 1-4. f_1 denotes the fraction of the first (narrower) Gaussian; σ_1 and σ_2 are the Gaussian widths. Errors shown for signal yields, f_1, σ_1 and σ_2 are statistical only.

Ξ_c decay mode	# of events	mass [MeV/ c^2]	f_1	σ_1 [MeV]	σ_2 [MeV]	$\chi^2/d.o.f.$
$\Xi_c^+ \rightarrow \Xi^- \pi^+ \pi^+$	628 ± 33	$2645.6 \pm 0.2_{-0.7}^{+0.6}$	0.43 ± 0.10	1.5 ± 0.3	4.7 ± 0.6	1.69
$\Xi_c^0 \rightarrow \Xi^- \pi^+$	638 ± 31	$2645.5 \pm 0.2_{-0.8}^{+0.7}$	0.56 ± 0.11	1.9 ± 0.3	5.3 ± 1.0	1.16
$\Xi_c^0 \rightarrow \Lambda K^- \pi^+$	549 ± 42	$2645.4 \pm 0.2_{-0.8}^{+0.7}$	0.32 ± 0.13	0.8 ± 0.1	3.6 ± 0.4	1.18
$\Xi_c^0 \rightarrow p K^- K^- \pi^+$	311 ± 27	$2645.3 \pm 0.2_{-0.7}^{+0.7}$	0.47 ± 0.07	1.0 ± 0.3	5.2 ± 1.0	0.93

As a cross-check, the same selection criteria as described above are also applied to MC samples: $e^+e^- \rightarrow c\bar{c}$ and $e^+e^- \rightarrow q\bar{q}$, $q = u, d, s$ with no signal decays included. The background shapes in the $\Xi_c\pi$ mass spectra for data and MC are in good agreements. The masses of $\Xi(2645)$, obtained from the signal MC sample, in which one of the decays 1-4 occurs in each individual event are in perfect agreement with the generated value of 2.64 GeV/ c^2 (the largest deviation is 0.2 ± 0.2 MeV/ c^2).

The systematic uncertainty of the $\Xi_c(2645)$ mass determination is evaluated as follows. First we consider systematic uncertainties related to the fit procedure. For each mode we modify the parameterization of the background (by varying values of parameters obtained from the Ξ_c sidebands by $\pm 1 \sigma$) and the mass range covered by the fit (extending it by 20%). The resulting change in the fitted masses are at most 0.1 MeV/ c^2 , depending on the decay. To take account of the imperfect understanding of the signal resolution, we perform fits varying the signal widths by their statistical errors, and compare with values where the widths are floated: the mass changes by 0.1 MeV/ c^2 .

The $\Xi_c(2645)$ mass also depends on the value of $m(\Xi_c)$ applied in the mass constraint fit. A change of $m(\Xi_c)$ almost linearly transforms to a shift of the measured $m(\Xi_c(2645))$. As a

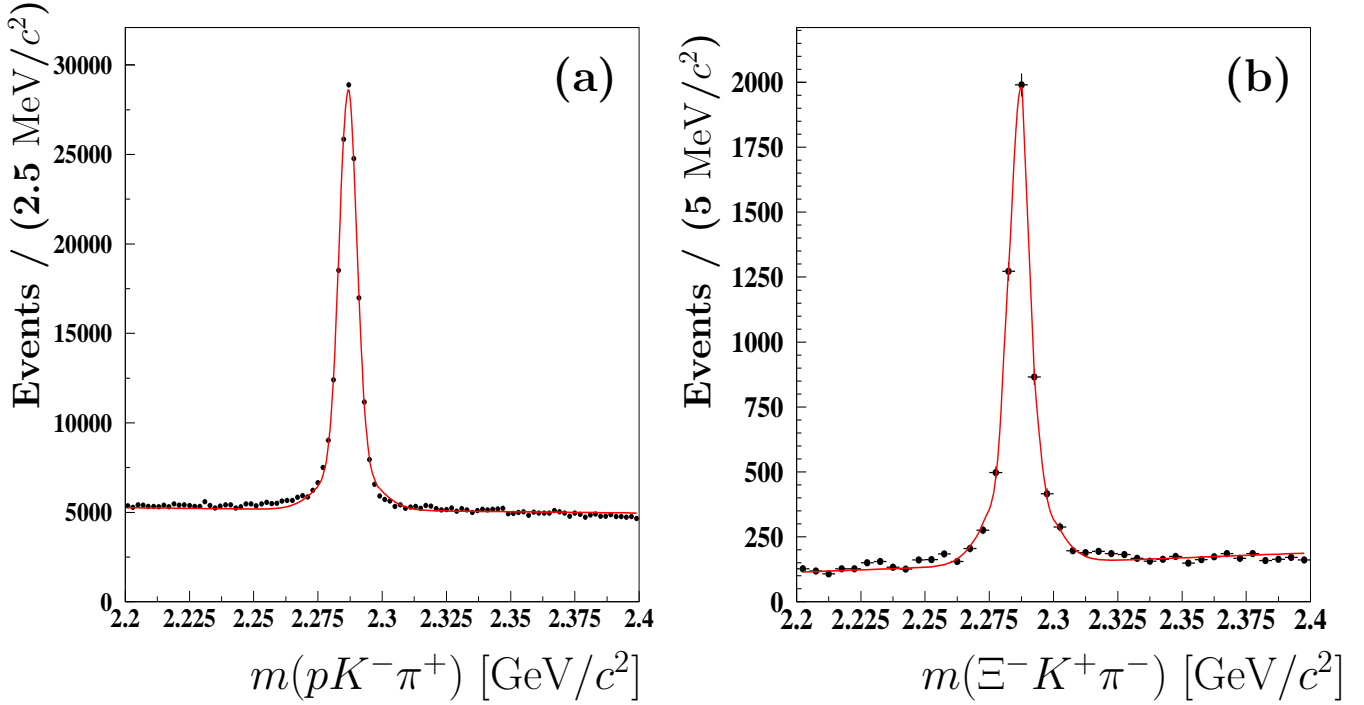


FIG. 4: Invariant mass distribution of selected $pK^-\pi^+$ (a) and $\Xi^-K^+\pi^+$ (b) combinations (solid histogram), together with the fit described in the text (curve).

result, we include a systematic uncertainty equal to the statistical error in the determination of the Ξ_c mass [15] i.e. $\pm 0.4 \text{ MeV}/c^2$ for the Ξ_c^+ and $\pm 0.6 \text{ MeV}/c^2$ for the Ξ_c^0 (cf Table I).

To test the modeling of the detector response (alignment, uniformness of magnetic field, correct treatment of specific ionization and scattering in the material), which could cause a bias in the overall mass scale, we study the $\Lambda_c^+ \rightarrow pK\pi$ and $\Lambda_c^+ \rightarrow \Xi^-K^+\pi^+$ decays. A fit to the $pK\pi$ invariant mass distribution (Fig. 4 (a)) yields $m(\Lambda_c) = 2286.74 \pm 0.02 \text{ MeV}/c^2$ (statistical error only). Here the signal is parameterized by a double Gaussian and the background is described by a first order polynomial. The above value is compared to the recent measurement by the BABAR collaboration [3] which yields $m(\Lambda_c) = 2286.46 \pm 0.14 \text{ MeV}/c^2$. As a result, a $-0.28 \text{ MeV}/c^2$ shift is assigned as a systematic error. Next the mass of Λ_c reconstructed in $pK\pi$ is also determined in bins of the azimuthal angle and the maximal deviations with respect to the value given above are assigned as the corresponding systematic errors, yielding $^{+0.17}_{-0.19} \text{ MeV}/c^2$. The same study, performed in bins of the Λ_c center-of-mass momentum provides an estimate of $\pm 0.09 \text{ MeV}/c^2$ as the respective systematic uncertainty.

To study the possible dependence of the $\Xi_c(2645)$ mass on the momentum and decay length of the Ξ^- and Λ hyperons (this may affect decay chains involving decays 1-3) we study the decay $\Lambda_c \rightarrow \Xi^-K^+\pi^+$. A fit to the $\Xi K\pi$ invariant mass distribution (Fig. 4(b)) yields $m(\Lambda_c) = 2286.63 \pm 0.09 \text{ MeV}/c^2$ (statistical error only). The Λ_c mass is also determined in bins of the momentum and decay length of the hyperon Ξ , which leads to systematic uncertainties of $^{+0.25}_{-0.27} \text{ MeV}/c^2$ and $^{+0.24}_{-0.30} \text{ MeV}/c^2$, respectively.

It was also checked that the measured mass value is stable within one standard deviation while fitting separately the spectra corresponding to particles and antiparticles in the final state. The total systematic uncertainty is obtained by adding the individual contributions in quadrature (Table III).

The average mass of the $\Xi_c(2645)^+$ is determined from the values given in Table II

TABLE III: Systematic uncertainties in the mass determination of the $\Xi_c(2645)$.

Systematic error [MeV/c ²]	Ξ_c final state			
	$\Xi^- \pi^+ \pi^+$	$\Xi^- \pi^+$	$\Lambda K^- \pi^+$	$p K^- K^- \pi^+$
(1) Signal width	0.1	0.1	0.1	0.1
(2) Fit range	0.0	0.0	0.0	0.0
(3) Background parameterization	0.1	0.0	0.0	0.0
(4) decay length of the $\Xi^- (\Lambda)$	+0.24 -0.30	+0.24 -0.30	+0.24 -0.30	0.0
(5) momentum of the $\Xi^- (\Lambda)$	+0.25 -0.27	+0.24 -0.30	+0.24 -0.30	0.0
(6) azimuthal angle dependence	+0.17 -0.19	+0.17 -0.19	+0.17 -0.19	+0.17 -0.19
(7) CMS momentum $p^*(\Xi_c(2645))$ dependence	0.09	0.09	0.09	0.09
(8) comparison to [3]	-0.28	-0.28	-0.28	-0.28
(9) mass constraint fit of the Ξ_c	0.4	0.6	0.6	0.6
Total systematic error	+0.6 -0.7	+0.7 -0.8	+0.7 -0.8	+0.6 -0.7

using the PDG unconstrained averaging algorithm [16] and assuming that all systematic uncertainties, apart from those related to the fit procedure, are common to the decay modes considered:

$$m_{\Xi_c(2645)^+} = (2645.4 \pm 0.1(\text{stat}) \pm 0.8(\text{syst})) \text{ MeV}/c^2, \quad (10)$$

and

$$m_{\Xi_c(2645)^0} = (2645.6 \pm 0.2(\text{stat})_{-0.7}^{+0.6}(\text{syst})) \text{ MeV}/c^2. \quad (11)$$

The above values are in agreement with, and more accurate than the current PDG averages (cf Table I).

Assuming that uncertainties (4)-(8) from the Table III are the same for charged and neutral $\Xi_c(2645)$'s and as such cancel in the $\Xi_c(2645)^+ - \Xi_c(2645)^0$ mass splitting, we find the mass difference between the charged and neutral states to be:

$$m_{\Xi_c(2645)^+} - m_{\Xi_c(2645)^0} = (-0.2 \pm 0.3(\text{stat}) \pm 0.7(\text{syst})) \text{ MeV}/c^2. \quad (12)$$

$\Xi_c(2815)$ MASS DETERMINATION

For each decay mode, we extract the signal yield and the $\Xi_c(2815)$ mass and width from a fit to the invariant mass distribution of $\Xi_c(2645)\pi$ pairs. We use a single Gaussian for the signals from $\Xi_c(2815)$ and $\Xi_c(2970)$. The background is parameterized by the threshold function (8). The fit results are summarized in Tables IV and V for the $\Xi_c(2815)$ and $\Xi_c(2970)$ signals, respectively.

The systematic uncertainties in the $\Xi_c(2815)$ mass determination were determined following the procedure used for the $\Xi_c(2815)$. The total systematic uncertainty is obtained by adding the individual contributions in quadrature (Table VI).

The average mass of the $\Xi_c(2815)^0$ is determined using the same method that was used for the $\Xi_c(2645)^+$. Again we assume that all systematic uncertainties, apart from those related to the fit procedure, are common to the decay modes considered:

TABLE IV: Signal yields and $\Xi_c(2815)$ masses and widths, obtained from the fits to the $\Xi_c(2645)\pi$ mass spectra for Ξ_c decays (1)-(4).

Ξ_c decay mode	# of events	mass [MeV/ c^2]	width [MeV]	$\chi^2/d.o.f.$
$\Xi_c^+ \rightarrow \Xi^- \pi^+ \pi^+$	65.6 ± 8.7	$2816.7 \pm 0.6(\text{stat})_{-0.8}^{+0.7}(\text{syst})$	3.8 ± 0.7	0.85
$\Xi_c^0 \rightarrow \Xi^- \pi^+$	39.8 ± 7.4	$2821.4 \pm 1.3(\text{stat})_{-1.0}^{+0.9}(\text{syst})$	5.8 ± 1.2	0.77
$\Xi_c^0 \rightarrow \Lambda K^- \pi^+$	41.0 ± 8.3	$2819.9 \pm 0.9(\text{stat})_{-1.0}^{+0.9}(\text{syst})$	3.5 ± 0.9	1.22
$\Xi_c^0 \rightarrow p K^- K^- \pi^+$	24.6 ± 5.9	$2818.8 \pm 0.9(\text{stat})_{-0.8}^{+0.8}(\text{syst})$	3.4 ± 0.9	1.22

TABLE V: Signal yields and $\Xi_c(2970)$ masses and widths, obtained from the fits to the $\Xi_c(2645)\pi$ mass spectra for Ξ_c decays (1)-(4).

Ξ_c decay mode	# of events	mass [MeV/ c^2]	width [MeV]
$\Xi_c^+ \rightarrow \Xi^- \pi^+ \pi^+$	77.0 ± 10.9	$2967.6 \pm 2.3(\text{stat})$	15 ± 2
$\Xi_c^0 \rightarrow \Xi^- \pi^+$	54.4 ± 9.3	$2964.9 \pm 2.3(\text{stat})$	12 ± 3
$\Xi_c^0 \rightarrow \Lambda K^- \pi^+$	100.2 ± 15.2	$2973.0 \pm 4.0(\text{stat})$	25 ± 5
$\Xi_c^0 \rightarrow p K^- K^- \pi^+$	35.6 ± 7.6	$2970.9 \pm 2.0(\text{stat})$	9 ± 2

TABLE VI: Systematic uncertainties in the mass determination of the $\Xi_c(2815)$.

Systematic error [MeV/ c^2]	Ξ_c final state			
	$\Xi^- \pi^+ \pi^+$	$\Xi^- \pi^+$	$\Lambda K^- \pi^+$	$p K^- K^- \pi^+$
(1) Signal width	0.3	0.5	0.4	0.4
(2) Fit range	0.1	0.0	0.1	0.1
(3) Background parameterization	0.0	0.2	0.1	0.0
(4) decay length of the $\Xi^- (\Lambda)$	$+0.24$ -0.30	$+0.24$ -0.30	$+0.24$ -0.30	0.0
(5) momentum of the $\Xi^- (\Lambda)$	$+0.25$ -0.27	$+0.24$ -0.30	$+0.24$ -0.30	0.0
(6) azimuthal angle dependence	$+0.17$ -0.19	$+0.17$ -0.19	$+0.17$ -0.19	$+0.17$ -0.19
(7) CMS momentum $p^*(\Xi_c(2645))$ dependence	0.09	0.09	0.09	0.09
(8) comparison to [3]	-0.28	-0.28	-0.28	-0.28
(9) mass constraint fit of the Ξ_c	0.4	0.6	0.6	0.6
Total systematic error	$+0.7$ -0.8	$+0.9$ -1.0	$+0.9$ -1.0	$+0.8$ -0.8

$$m_{\Xi_c(2815)^0} = (2819.7 \pm 0.8(\text{stat}) \pm 0.9(\text{syst})) \text{ MeV}/c^2, \quad (13)$$

and

$$m_{\Xi_c(2815)^+} = (2816.7 \pm 0.6(\text{stat})_{-0.8}^{+0.7}(\text{syst})) \text{ MeV}/c^2. \quad (14)$$

The above values are again in agreement with the PDG averages (cf. Table I). For the charged state the accuracy is comparable to the present PDG value, while for the neutral one it is better.

Assuming that uncertainties (4)-(8) from Table VI are the same for charged and neutral

$\Xi_c(2815)$ and as such cancel in the $\Xi_c(2815)^+ - \Xi_c(2815)^0$ mass splitting, we find the mass difference between the charged and neutral states to be

$$m_{\Xi_c(2815)^+} - m_{\Xi_c(2815)^0} = (-3.0 \pm 1.0(\text{stat}) \pm 0.8(\text{syst})) \text{ MeV}/c^2. \quad (15)$$

CONCLUSIONS

Based on the large sample of the Ξ_c hyperons, reconstructed in four exclusive decays (of which the decay $\Xi_c(2815) \rightarrow \Xi_c(2645)\pi$ is observed for the first time), the masses of $\Xi_c(2645)$ and $\Xi_c(2815)$ baryons, together with the respective mass splittings, are measured to be

$$\begin{aligned} m_{\Xi_c(2645)^+} &= (2645.4 \pm 0.1(\text{stat}) \pm 0.8(\text{syst})) \text{ MeV}/c^2, \\ m_{\Xi_c(2645)^0} &= (2645.6 \pm 0.2(\text{stat})_{-0.7}^{+0.6}(\text{syst})) \text{ MeV}/c^2, \\ m_{\Xi_c(2645)^+} - m_{\Xi_c(2645)^0} &= (-0.2 \pm 0.3(\text{stat}) \pm 0.7(\text{syst})) \text{ MeV}/c^2, \\ m_{\Xi_c(2815)^+} &= (2816.7 \pm 0.6(\text{stat})_{-0.8}^{+0.7}(\text{syst})) \text{ MeV}/c^2, \\ m_{\Xi_c(2815)^0} &= (2819.7 \pm 0.8(\text{stat}) \pm 0.9(\text{syst})) \text{ MeV}/c^2, \\ m_{\Xi_c(2815)^+} - m_{\Xi_c(2815)^0} &= (-3.0 \pm 1.0(\text{stat}) \pm 0.8(\text{syst})) \text{ MeV}/c^2, \end{aligned}$$

with a much better precision than the current world averages.

We thank the KEKB group for the excellent operation of the accelerator, the KEK cryogenics group for the efficient operation of the solenoid, and the KEK computer group and the National Institute of Informatics for valuable computing and Super-SINET network support. We acknowledge support from the Ministry of Education, Culture, Sports, Science, and Technology of Japan and the Japan Society for the Promotion of Science; the Australian Research Council and the Australian Department of Education, Science and Training; the National Science Foundation of China and the Knowledge Innovation Program of the Chinese Academy of Sciences under contract No. 10575109 and IHEP-U-503; the Department of Science and Technology of India; the BK21 program of the Ministry of Education of Korea, the CHEP SRC program and Basic Research program (grant No. R01-2005-000-10089-0) of the Korea Science and Engineering Foundation, and the Pure Basic Research Group program of the Korea Research Foundation; the Polish State Committee for Scientific Research; the Ministry of Science and Technology of the Russian Federation; the Slovenian Research Agency; the Swiss National Science Foundation; the National Science Council and the Ministry of Education of Taiwan; and the U.S. Department of Energy.

-
- [1] R. Chistov et al., preprint hep-ex/0606051 (2006); submitted to *Phys. Rev. Lett.*.
 - [2] R. Mizuk et al., preprint BELLE-CONF-0602 (2006); contribution no. 602 to ICHEP06.
 - [3] B. Aubert et al., (BABAR Collaboration), *Phys. Rev.* **D 72**, 052006 (2006).
 - [4] B. Aubert et al., (BABAR Collaboration), preprint SLAC-PUB-11786, hep-ex/0603052 (2006), subm. to *Phys. Rev. Lett.*.
 - [5] T. Lesiak *et al.*, (Belle Collaboration), *Phys. Lett.* **B 605**, 237 (2004) and *Phys. Lett.* **B 617**, 198 (2005) (erratum).

- [6] S. Capstick, N. Isgur, *Phys. Rev. D*, **34**, 2809 (1986);
Yong-seok Oh, Byung-Yoon Park, *Phys. Rev. D*, **53**, 1605 (1996).
- [7] N. Isgur, M.B. Wise, *Phys. Rev. Lett.*, **66**, 1130 (1991).
- [8] Charge conjugate modes are implicitly included everywhere, unless specified otherwise.
- [9] S. Eidelman et al., *Phys. Lett. B*, **592**, 1 (2004) and 2005 partial update (URL: <http://pdg.lbl.gov/>).
- [10] S. Kurokawa and E. Kikutani, *Nucl. Instrum. Methods A*499 (2003) 1, and other papers included in this Volume.
- [11] A. Abashian *et al.*, (Belle Collaboration), *Nucl. Instr. and Meth. A* **479**, 117 (2002).
- [12] R.E. Kalman, *Trans. Am. Soc. Mech. Eng. D*. **82** (1960) 35;
R.E. Kalman and R.S. Bucy., *ibid.* **83** (1961) 95.
- [13] The z -axis is oriented opposite to the direction of the e^+ beam, along the symmetry axis of the detector.
- [14] For protons attributed to the decay $\Lambda \rightarrow p\pi$, the hadron identification criterion was relaxed to relative to with the one described in the section “Track reconstruction and identification”.
- [15] Here we use the symmetric errors of the “fit” value of Table I; the (larger) asymmetric errors on the “average” value are dominated by the mass scale uncertainty of our previous measurement [5], which is estimated more thoroughly in this study.
- [16] S. Eidelman et al., *Phys. Lett. B*, **592**, 1 (2004); introduction, pp. 14-16.